www.czasopisma.pan.pl PAN www.journals.pan.pl
Chemical and Process Engineering 2018, 39 (4), 427–448
DOI: 10.24425/122961

SORPTION-ENHANCED STEAM METHANE REFORMING (SE-SMR) – A REVIEW: REACTOR TYPES, CATALYST AND SORBENT CHARACTERIZATION, PROCESS MODELING

Robert Cherbański, Eugeniusz Molga*

Faculty of Chemical and Process Engineering, Warsaw University of Technology, ul. Waryńskiego 1, 00-645 Warszawa, Poland

Dedicated to Professor Andrzej Burghardt on the occasion of his 90th birthday

In this review, research carried out on sorption-enhanced steam methane reforming (SESMR) process is presented and discussed. The reactor types employed to carry out this process, fixed packed bed and fluidized bed reactors, are characterized as well as their main operating conditions indicated. Also the concepts developed and investigations performed by the main research groups involved in the subject are summarized. Next the catalysts and CO_2 sorbents developed to carry out SE-SMR are characterized and the relationships describing the reaction and sorption kinetics are collected. A general approach to model the process is presented as well as results obtained for a calculation example, which demonstrate the main properties of SE-SMR.

Keywords: reactive adsorption, adsorptive reactors, reactor modeling, sorption-enhanced reaction process (SERP), steam methane reforming (SMR)

1. INTRODUCTION

Hydrogen is a fundamental raw material in numerous chemical syntheses [1] as it is widely used as an important reagent in chemical industry. In the so called "hydrogen economy" it is also provided as a universal energy carrier. Hydrogen can be obtained from renewable energy resources, such as bioethanol, glycerol, bio-oil and from biomass - although nowadays, hydrogen is mainly produced from fossil fuels. More than 50% of the global hydrogen production is provided by methane steam reforming, while 30% is obtained from oil/naphtha reforming and 18% from coal gasification [2].

In a SMR process the conversion of methane to hydrogen can be represented with the following set of reversible reactions:

$$CH_4 + H_2O \leftrightarrow CO + 3H_2 \qquad \Delta H = +206\ \mathrm{kJ/mol} \tag{1}$$

$$CH_4 + 2H_2O \leftrightarrow CO_2 + 4H_2 \qquad \Delta H = +165\ \mathrm{kJ/mol} \tag{2}$$

These reactions are usually carried out at a temperature above 750 °C and at a pressure of 14–20 bar. Due to their reversibility, a complete conversion of methane is not possible, additionally the obtained hydrogen

* Corresponding author, e-mail: eugeniusz.molga@pw.edu.pl

requires purification, as the product gas contains even 8–10% of CO on a dry basis (e.g see Hufton *et al.* [3]). Therefore an auxiliary process such as water-gas shift (WGS) reaction is required:

$$CO + H_2O \leftrightarrow CO_2 + H_2 \qquad \Delta H = -41 \text{ kJ/mol} \tag{3}$$

So, the effluent gas form the reformer is fed to the WGS reactor, where a much lower temperature of 300–400 °C is kept.

Integration of reversible chemical reactions with *in-situ* sorption of one product helps to improve the reactant conversion and simultaneously, due to removal of one product from the reaction zone, a purity of the demanded product in the outlet stream can be also augmented. Such an integrated process, which incorporates both the chemical reaction and the separation by sorption processes, is called the *reactive adsorption process* or the *sorption enhanced reaction process* (SERP) and is now well characterized in the literature of the subject – e.g. see [4–9].

In the considered (MSR + WGS) process, an integration of chemical reactions with simultaneous sorption of CO_2 improves methane conversion and simultaneously the purity of produced hydrogen. *In-situ* adsorption of CO_2, which is the main co-product of SMR, shifts the equilibrium of reactions (2 and 3) to the right, so almost total conversion of the CO produced in reaction (1) is possible, also a conversion of methane in reactions (1) and (2) is much larger than that obtained at the equilibrium conditions. The process, merging the reaction and *in situ* adsorption of one product, known as sorption-enhanced steam methane reforming (SESMR) has been widely investigated and developed starting from the late 1990s.

Experimental results collected from adsorptive reactors as well as from numerical simulations indicate that at operating conditions which are more moderate in comparison to those applied in the conventional methane reformer – i.e. at the temperature of 450–490 °C and pressure of 180–890 kPa – the gas product contains 90–98% of H_2, with methane as a prime impurity accompanied with traces of CO_2 (less than 400 ppm) and CO (below 50 ppm) [10, 11].

Numerous papers devoted to the application of reactive adsorption in production of pure hydrogen by sorption-enhanced steam-methane reforming (SE-SMR) can be found in the literature of the subject – starting from the pioneering papers [12–16]. While among the most recent publications the following contributions, which indicate also the main institutions and research groups involved in the subject, should be mentioned [11, 17, 26–35, 18, 36–45, 19, 46–52, 20–25].

The aim of this review is to present and discuss a summary of the research carried out on the sorption-enhanced steam methane process used for production of pure hydrogen. Also types of reactors employed to perform SE-SMR processes, catalysts and sorbents are characterized.

It should be pointed out that not all papers published on the subject have been cited in this review, as it is really impossible due to a huge number of contributions. However, our intention was to present the most representative results published on this subject.

Also our own concept to improve the considered SE-SMR process by application of fly ashes (FA) originating from power plants and combined heat and power plants as an active CO_2 sorbent is presented and characterized.

2. REACTORS EMPLOYED TO CARRY OUT SESMR

SESMR is usually carried out in a one-stage multifunctional reactor of special type, called the adsorptive reactor [4–6], in which chemical reactions and *in situ* sorption of produced CO_2 are merged. The principle of the process is shown in Fig. 1, where the reactor active packing consists of the catalyst and sorbent particles.

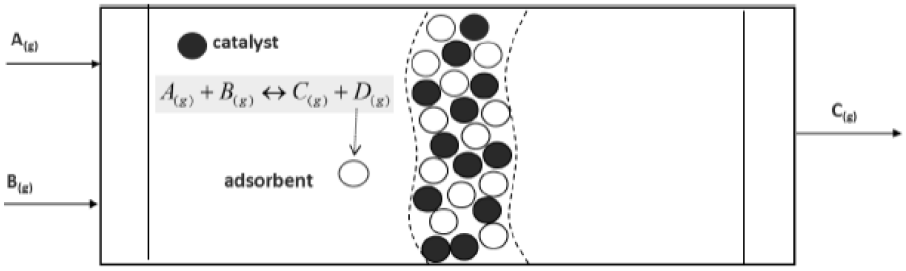

Fig. 1. The principle of operation of the adsorptive reactor

However, in some practical solutions, the use of bi-functional (or generally called multifunctional) packing grains is proposed, in which structured grains play simultaneously the catalyst as well as the CO_2 sorbent roles – e.g. see [53–55]. Sometimes, a more complex or special configuration of the reactor bed is employed – including the number of subsections each with different adsorbent to catalyst mass ratio [19–21]. In this approach, called also the subsection controlling strategy [20], three subsections in the adsorptive reactor column can be distinguished, each with different adsorbent to catalyst ratio and also a different reactor wall temperature within the chosen section(s) can be applied. Also the tandem bed configuration was proposed [28], where different types of sorbents are placed in an upstream and a downstream section of the bed, respectively.

The adsorptive reactor shown in Fig. 1 is based on the fixed packed bed concept [11, 17, 26–35, 18, 36–38, 19–25], while in numerous papers binary fluidized bed reactors are also described in which cyclic operation of the reforming process and the sorbent calcination is investigated [39–43, 48–52].

As each CO_2 sorbent employed in the SESMR process has a limited capacity, in the entire installation for hydrogen production two steps can be distinguished; in the first one methane is converted and produced CO_2 simultaneously adsorbed, while in the second one the sorbent is regenerated and CO_2 released (desorbed).

In packed bed reactors a cyclic operation is carried out – i.e. just before a complete saturation of sorbent with CO_2, the feed of CH_4/H_2O is switched off, then the bed is heated up and the sorbent regenerated, so the sequential operating mode is used. Therefore, a battery of reactors working in parallel can be employed and the simplest configuration consisting of two reactor columns is shown in Fig. 2. Notice that

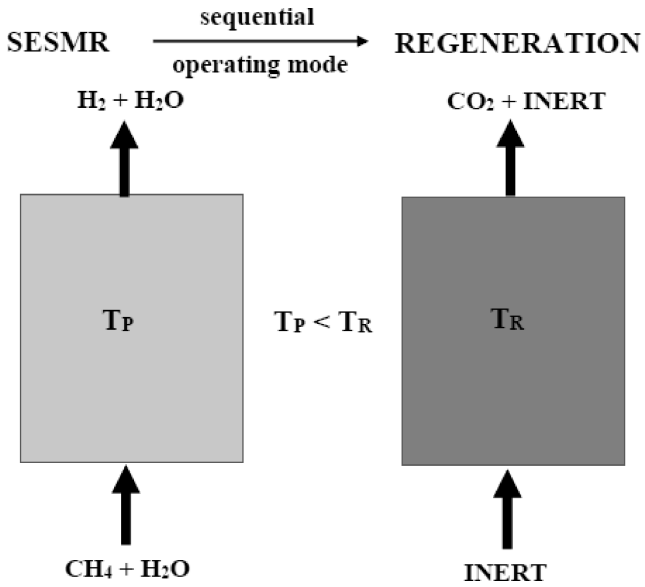

Fig. 2. Configuration of cyclic process carried out in the fixed packed bed reactor (SESMR process) and operating sequentially the sorbent regenerator. T_P – SESMR process temperature, T_R – regeneration temperature

the regeneration temperature – T_R (usually 800–1000 °C) is significantly higher than the SESMR process temperature – T_P (480–580 °C).

In circulating fluidized bed reactors, a system of two fluidization columns (reactor-regenerator system) operating simultaneously is applied– see Fig. 3. The solid phase consisting of the catalyst and sorbent fine particles, is circulated between the reactor and the sorbent regenerator unit. The reactor operates in the bubbling fluidization state, while the regenerator in the fast fluidization state [42]. Also in this case the temperature – T_R is higher than T_P.

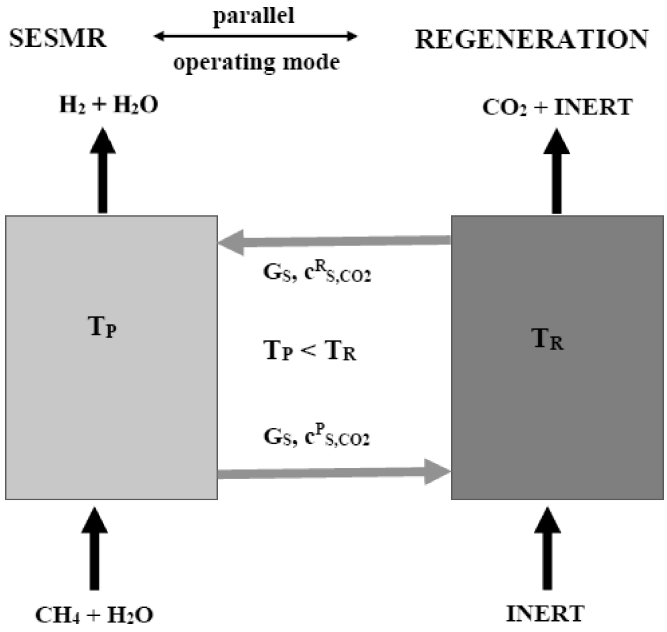

Fig. 3. Configuration of continuous steady-state process carried out in fluidized bed reactor (SESMR process) and operating in parallel the sorbent regenerator. T_P – SESMR process temperature, T_R – regeneration temperature, G_S – flux of solids circulating between reactor and regenerator, $c^P_{S,CO2}$, $c^R_{S,CO2}$ – CO_2 concentration in sorbent solids leaving the reactor and the regenerator, respectively

A comprehensive review of methods applied for hydrogen production from fossil fuels with simultaneous CO_2 capture was recently given in the paper by Voldsund et al. [56], which contains characterization of reforming or gasification with subsequent gas separation by adsorption, absorption, membrane or cryogenic separation.

A more detailed characterization of reactor types employed to carry out SESMR can be found in contributions cited below. In a series of papers [11, 17–23] the results of a wide-ranging research program carried out at the LSRE of Porto University (Portugal) are reported – including experimental and simulation investigations, conceptual parametric studies, process modeling with validation of model predictions, controlling strategies as well as an application of improved CO_2 hydrotalcite-like sorbents. The state-of-the-art has been recently summarized in a comprehensive publication [9].

A remarkable impact on the subject was given also by a group from the Eindhoven University of Technology (the Netherlands), who in a series of publications [34–38] reported their modeling and experimental results. These papers present a fundamental approach to modeling of SESMR processes with highly active catalysts and different CO_2 sorbents [34, 37, 38], validated with appropriate experimental results [35, 36].

The next research group from Trondheim (Norway) [24–27] was busy mainly with the use of lithium oxides as CO_2 acceptors in the SESMR process, while a group from Petten (the Netherlands) [28–33] gave a complete analysis of the process – from thermodynamic considerations and special bed configuration to modeling of the process and its verification.

The group from the Norwegian University of Science and Technology (Trondheim, Norway) in numerous papers [39, 40, 49–52, 41–48] reported also the results obtained mainly for SESMR process carried out in fluidized bed reactors and presented a numerical model formulation, simulations of reactor operation, numerical investigations of gas-solid hydrodynamic behavior [49], an influence of catalyst and sorbent properties on the reactor performance [45] as well as parameter sensitivity [46].

A summary of the reactor types employed to carry out the SESMR process and their main operating conditions are given in Table 1.

Table 1. Summary of reactor types employed to carry out the SESMR process and their main operating conditions

Reactor type	Catalysts	CO_2 sorbents	Process temperature/ Pressure [°C] / [MPa]	Experimental/ Simulations/ Special arrangements	Ref.
FixBR		hydrotalcite-based	450–490/ 0.22–0.89	Numerical simulations/ Intraparticle limitations	[11]
FixBR	Ni-based	hydrotalcite-based	428–467/ 0.31–0.72	Experiments/ Numerical simulations	[15]
FixBR	Ni-based	hydrotalcite-based	500/ 0.1–0.5	Numerical simulations/ Two-section reactor	[19]
FixBR	Ni-based	hydrotalcite-based	400–490/ 0.2–0.44	Numerical simulations/ Subsection controlling strategy	[20, 21]
FixBR	Ni-based	hydrotalcite-based	450/ 0.45	Numerical simulations/ Five-steps one-bed strategy	[22, 23]
FixBR	Ni-based (two types)	K-modified HTC	505/ 0.2–0.4	Experiments/ Numerical simulations	[57]
FixBR	Ni-based	CaO	660–750/ 0.3–1.5	Experiments/ Numerical simulations	[58]
FixBR/ FluBR	Ni-based	Li_4SiO_4, $LiZrO_3$	575/ 1–2	Numerical simulations	[24, 25]
FixBR	Ni-based	CaO, Li_4SiO_4, Li_2ZrO_3, K-dopped, Na_2ZrO_3	575/ 1–2.5	Numerical simulations	[26, 27]
FixBR	Rh-based	HTCs (hydrotalcities)	400/ 0.1	Numerical simulations	[29, 30]
FixBR	$Rh/Ce_\alpha Zr_{1-\alpha}O_2$	K-promoted hydrotalcite, Li_2ZrO_3	450–600/ 0.46–1.5	Experiments/ Numerical simulations	[34–36]
FixBR	Ni/MgO	K-promoted hydrotalcite, Li_2ZrO_3	500/0.46	Numerical simulations	[37, 38]
FluBR	Ni-based	CaO-based	575–600–627/ 0.10–1.5	Numerical simulations	[39, 41, 43–50]
FixBR	Ni/γ-Al_2O_3	K2CO3 – doped – Li_4SiO_4	450–650	Experiments/ Numerical simulations/ Sorbent regeneration	[59]
GSSTFR	Ni/γ-Al_2O_3	FA	300–500/ 0.2–0.8	Experiments/ Numerical simulations	[60]
FluBR	Ni/γ-Al_2O_3	FA	300–500/ 0.2–0.8	Numerical simulations	this work

The papers cited above deal usually with the SESMR process, although in some of them the entire process is described, which includes also a strategy of sorbent regeneration. Mostly multistep pressure swing regeneration (PSR) is applied, although temperature (thermal) swing regeneration (TSR) and concentration swing regeneration (CSR) processes are also employed.

A comprehensive survey of cyclic hydrogen production processes is given by Wu et al. [7], where an influence of operating conditions, type of feedstock, catalyst and sorbent type as well as sorbent regeneration method on the product quality is summarized.

Recently, an application of the gas-solid-solid trickle flow reactor (GSSTFR) to carry out a continuous SESMR process with simultaneous sequestration of CO_2 on fly ashes was considered [60]. In such an approach the catalyst active sites can be immobilized on the fixed carrier of large pore size, while fine particles of sorbent (fly ashes) flow downwards through the voids. Gas can flow downwards (co-currently to the fly ashes stream) or upwards (counter-currently).

An idea of the gas-solid-solid trickle flow reactor (GSSTFR) was firstly proposed by Westerterp and Kuczyński [61, 62] to carry out the integrated sorption enhanced process with equilibrium reaction – namely the methanol synthesis. This idea was later developed and demonstrated in more recent contributions to be applied in: – methane oxidation to methanol [63], – industrial size reactor for methanol synthesis [64], – dimethyl ether synthesis [65] and Fischer-Tropsch synthesis [66]. The obtained results indicate a feasibility of the proposed approach as well as an increase of process productivity in comparison to the conventional solutions. Therefore, it seems that an application of GSSTFR to carry out the considered SESMR process with simultaneous sequestration of CO_2, could be quite effectively implemented in industrial scale, as currently numerous commercial solutions for open cell metallic and ceramic foams with "tailored" structure (void size and their tortuosity) can be found [67, 68].

3. MODELING OF SESMR PROCESS

3.1. Catalyst and the reaction kinetics

The catalysts used for SMR and SESMR processes are very well established. Mostly commercial nickel based catalysts on Al_2O_3 support are employed [69], but different types of active metals, additives and supports are also considered. Among others papers [34, 35, 70] a novel, highly active $Rh/Ce_\alpha Zr_{1-\alpha}O_2$ catalyst was characterized and used to carry out SESMR process. Also many studies have been carried out with nickel catalysts on different supports to increase their thermal stability and/or activity – e.g. see papers [71, 72], where ZrO_2, $Ce\text{-}ZrO_2$ supports are investigated or paper [73], where addition of Zr to the Ni/SiO_2 catalyst for improvement of steam resistance is reported. Some papers [53, 54, 57, 69, 70, 74] on catalysts used for SESMR should be here also mentioned.

The intrinsic kinetics of steam methane reforming (SMR) process represented by a set of reversible reactions shown in Eqs. (1)–(3), has been described by Xu and Froment [75], who for a nickel catalyst supported on MgO/Al_2O_3 proposed expressions enabling estimation of appropriate reaction rates. For each reaction listed in Eqs. (1)–(3) the appropriate rate expressions read as follows:

$$r_{\mathrm{I}} = \frac{1}{M^2} \cdot \frac{k_{\mathrm{I}}}{p_3^{2.5}} \left(p_1 \cdot p_2 - \frac{p_3^3 \cdot p_5}{K_{\mathrm{I}}} \right) \tag{4}$$

$$r_{\mathrm{II}} = \frac{1}{M^2} \cdot \frac{k_{\mathrm{II}}}{p_3^{3.5}} \left(p_1 \cdot p_2^2 - \frac{p_3^4 \cdot p_4}{K_{\mathrm{II}}} \right) \tag{5}$$

$$r_{\mathrm{III}} = \frac{1}{M^2} \cdot \frac{k_{\mathrm{III}}}{p_3} \left(p_5 \cdot p_2 - \frac{p_3 \cdot p_4}{K_{\mathrm{III}}} \right) \tag{6}$$

where the value M appearing in denominators of these equations is equal to:

$$M = 1 + K_5 \cdot p_5 + K_3 \cdot p_3 + K_1 \cdot p_1 + \frac{K_2 \cdot p_2}{p_3} \tag{7}$$

The kinetic and sorption constants appearing in the kinetic expressions of Eqs. (4)–(7) as well as their temperature dependencies are shown in Table 2.

Table 2. Kinetic and sorption constants appearing in the kinetic expressions of Eqs. (4)–(7) [75]

$$K_1 = 0.179 \exp\left(\frac{38280}{R}\left(\frac{1}{T} - \frac{1}{823}\right)\right) \tag{8}$$

$$K_2 = 0.4152 \exp\left(\frac{-88680}{R}\left(\frac{1}{T} - \frac{1}{823}\right)\right) \tag{9}$$

$$K_3 = 0.0296 \exp\left(\frac{82900}{R}\left(\frac{1}{T} - \frac{1}{648}\right)\right) \tag{10}$$

$$K_5 = 40.91 \exp\left(\frac{70650}{R}\left(\frac{1}{T} - \frac{1}{648}\right)\right) \tag{11}$$

$$K_{\mathrm{I}} = 4.707 \times 10^{12} \exp\left(\frac{-224000}{R \cdot T}\right) \tag{12}$$

$$K_{\mathrm{III}} = 1.142 \times 10^{-2} \exp\left(\frac{37300}{R \cdot T}\right) \tag{13}$$

$$K_{\mathrm{II}} = K_{\mathrm{I}} K_{\mathrm{III}} \tag{14}$$

$$k_{\mathrm{I}} = 1.842 \times 10^{-1} \exp\left(\frac{-240100}{R}\left(\frac{1}{T} - \frac{1}{648}\right)\right) \tag{15}$$

$$k_{\mathrm{II}} = 2.193 \times 10^{-2} \exp\left(\frac{-243900}{R}\left(\frac{1}{T} - \frac{1}{648}\right)\right) \tag{16}$$

$$k_{\mathrm{III}} = 7.558 \times 10^{3} \exp\left(\frac{-67130}{R}\left(\frac{1}{T} - \frac{1}{648}\right)\right) \tag{17}$$

3.2. Sorbents and sorption kinetics

An intensive research on sorbents, which can be appropriate to carry out SESMR processes effectively, is still in progress. In general, at the operating conditions of SESMR process, the sorbent has to be highly selective towards CO_2 and the sorption rate should be compatible to the reaction rate – i.e. to the rate of CO_2 production. Additionally, these sorbents should have a sufficiently high sorption capacity as well as – due to their multiple cyclic regeneration - mechanical, thermal and chemical durability. A lot of contributions dealing with investigations of CO_2 sorbents can be found in the literature and some fundamental conclusions can be grouped as follows:

- CaO (lime) as well as alkali-modified hydrotalcites are mostly used as efficient sorbents for CO_2 capture during SESMR process [17–19, 36, 37, 58, 76, 77]. Ca-based sorbents are specially advantageous due to their low cost, availability, high CO_2 capacity and good sorption kinetics. However, they are unstable in long-term sorption-desorption operations due to sintering [78, 79]. Therefore, a lot of investigations are still carried out to improve their durability in cyclic operation by addition of various precursors and different treatment, although results obtained are sometimes contradictory [78],

- lithium oxides and lithium containing materials (mainly Li_2ZrO_3, K-doped Li_2ZrO_3 and Li_4SiO_4) are also considered as an effective alternative, due to their stability and good sorption kinetics, although they suffer from a relatively small CO_2 capacity [24–27, 59, 78],
- in order to eliminate mass transfer resistances hybrid catalyst-sorbent structured systems are proposed and investigated. However, most of proposals are just conceptual and a more practical approach and results are still expected [78].

The latest reviews on high temperature CO_2 sorbents and their applications for hydrogen production should be here mentioned [78, 79], in which a complete scope of the subject is given. Also some attempts to apply activated carbons for purification of hydrogen obtained from conventional steam methane reforming process should be here mentioned [80].

The main problem in practical application of the integrated SESMR process is a limited sorption capacity of used sorbents, so after their saturation with CO_2 the process has to be stopped and a regeneration of sorbent accomplished. Such a cyclic operation of adsorptive reactors makes the process complex, increases exploitation costs and generates special requirements for sorbents. It should be pointed out that desorption of CO_2 from a saturated CaO-based sorbent ($CaCO_3$) and regeneration of this sorbent is usually carried out at the temperature as high as 900–1000 °C. Taking above into account, an application of fly ashes (FA) originating from power plants seems to be a promising concept. Because fly ashes - abundantly available industrial wastes - are very cheap, practical aspects of their use in the SESMR process is related to the fact that after full or partial saturation with CO_2 they do not have to be regenerated and can be even further utilized in a building industry or directly in road construction and in mines [60, 81–84]. So, through the use of fly ashes as CO_2 acceptors, an economic efficiency of the hydrogen production can be significantly improved. Additionally, all CO_2 emitted during the hydrogen production process is sequestrated. So, an application of fly ashes in the SESMR process helps to reduce emission of CO_2 and in consequence improves ecological factors of hydrogen production.

Recently, the use of fly ashes as a basic component of CO_2 sorbents has quite widely been discussed in the literature [82–89]. Because FA contain significant amounts of Al_2O_3, SiO_2, CaO, MgO as well as other alkali components they receive an increasing interest as precursors for high temperature CO_2 sorbents [81, 84, 87, 89]. Numerous successful attempts should be here pointed out – e.g. those to produce a novel lithium-based sorbent [83], elaboration of wet and dry technologies for CO_2 capture [82, 84], utilization of the stabilizing effect of FA on Ca-based sorbents for cyclic CO_2 sorption [85], development of sodium-lithium-FA sorbents [86] as well as sodium and potassium –based FA sorbents [87, 88], development of standardized production for blended CO_2 sorbents containing CaO, MgO and FA to improve their effectiveness and stability [89].

However, to improve significantly the SESMR process applied for hydrogen production, an elimination of the CO_2 sorbent regeneration step is crucial. From this point of view, any modifications of fly ashes, which generate additional significant costs are not productive as an expensive sorbent has to be regenerated. Taking above into account, some successful investigations have been carried out to check a direct applicability of FA for CO_2 sorption in the SESMR process. In our previous study some promising results of these investigations have been presented [82]. As FA used in these investigations originated from a combined heat and power plant, where flue gases were desulphurized using calcium methods, the CaO content in used FA was augmented by 10% [81, 82]. For investigated FA, a sufficiently high sorption rate and sorption capacity for the CO_2 has been found [82]. Summarizing, an application of fly ashes can help to reduce emission of CO_2 and simplifies the process, so in consequence improves economic and ecological factors of hydrogen production. However, for practical implementation of a method employing FA in the industrial scale, a lot of practical problems have to be still solved – e.g. those related to continuous feeding of the reformer with a fresh FA stream and removal of spent FA saturated with CO_2, an effective contact of both solid phases (sorbent and catalyst) with the gas phase etc.

An experimental proof of successful application of fly ashes in the SESMR process was provided by Cherbański and Molga [60], who also gave some indications for industrial implementation of this approach.

In modeling of adsorptive reactors, except for estimation of reaction rates, also a prediction of CO_2 sorption rate is crucial.

In the considered SESMR processes a selective sorption of CO_2 is assumed, so sorption rates and solid phase concentrations of other components (CH_4, H_2O, H_2 and CO) are always equal to zero.

For CaO-based sorbents the unreacted core model can be used to predict sorption (chemisorption) rates [82]. The representative results for this kind of sorbent are summarized with the following carbonation rate equation [58]:

$$r_{S,\mathrm{CaO}} = \frac{1}{M_{\mathrm{CaO}}} \frac{k_c}{(b+t)^2} \exp\left(\frac{-28882}{R \cdot T}\right) \tag{18}$$

Then, neglecting the short initial period, the CO_2 sorption rate can be estimated with the expression:

$$r_{S,4} = 24.1 \times 10^3 \exp\left(\frac{-12171}{T}\right) \tag{19}$$

Molga and Cherbanski [82] published a detailed report on CO_2 sorption rate on fly ashes (FA) originating from power plants. It has been found that, similarly to CO_2 sorption on CaO grains [58], also for FA the sorption rate is a zero order with respect to CO_2 – i.e. the observed sorption (chemisorption) rate does not depend on the CO_2 concentration in the gaseous phase. Further, the analysis carried out with use of unreacted core model have indicated, that for CO_2 sorption on FA the internal mass transfer resistances can be neglected. So, the specific CO_2 sorption rate expressed per mass unit of fly ashes can be estimated only as a temperature dependent with the following Arrhenius type equation [82]:

$$r_{S,\mathrm{FA}} = 72.1 \times 10^{-3} \exp\left(\frac{-28882}{R \cdot T}\right) \tag{20}$$

From performance point of view, for any sorption process the CO_2 uptake coefficient – γ is a very important parameter which describes a degree of sorbent saturation with CO_2 and is defined as:

$$\gamma = \frac{m_{\mathrm{CO2}}}{m_{\mathrm{FA}}} \tag{21}$$

where the mass of sequestrated CO_2 – m_{CO2}, which depends on the sorption time – t_S, can be estimated from the following relationship:

$$m_{\mathrm{CO2}} = M_{\mathrm{CO2}} \cdot m_{\mathrm{FA}} \int_0^{t_S} r_{S,\mathrm{FA}}\, dt \tag{22}$$

It has been found [82], that the maximum sorption capacity of FA sorbent is equal to $\gamma_{\mathrm{max,FA}} = 0.078$ $\mathrm{kg_{CO2}/kg_{FA}}$, although in technical applications this estimated maximum value $\gamma_{\mathrm{max,FA}}$ should be replaced by a more realistic one: $\gamma_{\mathrm{sat}} = 0.035$ $\mathrm{kg_{CO2}/kg_{FA}}$, which is fully compatible with sorption capacities obtained for other CO_2 sorbents – e.g. for hydrotalcities [18].

It should be pointed out, that in the case of chemisorption (on CaO, FA) the appropriate rates of CO_2 sorption can be directly estimated from Eqs. 19 and 20, respectively. While for physical sorption (e.g. on hydrotalcites) to estimate the CO_2 sorption rate the linear driving force model is usually applicable [16]:

$$r_S = k_{S,\mathrm{CO2}} \left(q_{\mathrm{CO2},eq} - \overline{q}_{\mathrm{CO2}}\right) \tag{23}$$

where the sorption rate constant – $k_{S,\mathrm{CO2}}$ can be estimated with temperature dependent expressions [17].

To determine the equilibrium concentration $q_{CO2,eq}$ the Langmuir and bi-Langmuir models can be applied. The Langmuir model reads as follows [14]:

$$q_{CO2,eq} = \frac{m_{CO2} \cdot b_{CO2} \cdot p_{CO2}}{1 + b_{CO2} \cdot p_{CO2}} \tag{24}$$

where the constants m_{CO2} and b_{CO2} can be found easily in the literature – e.g. for hydrotalcite-like sorbents in the papers [14, 20]. The bi-Langmuir model takes into account two different types of sorption sites [17] – those responsible for physical and chemical sorption. This reads as follows:

$$q_{CO2,eq} = q_{max,1} \frac{K_{eq,1} \cdot p_{CO2}}{1 + K_{eq,1} \cdot p_{CO2}} + q_{max,2} \frac{K_{eq,2} \cdot p_{CO2}}{1 + K_{eq,2} \cdot p_{CO2}} \tag{25}$$

where the constants $K_{eq,1}$ and $K_{eq,2}$ as well as $q_{max,1}$ and $q_{max,2}$ can be estimated following the relationships given by Chanburanasiri et al. [17].

3.3. Calculation example for modeling a fluidized bed gradientless reactor (FBGLR)

In the literature of the subject, numerous papers have been published on modeling of SESMR process carried out in reactors of different types. Most of them are devoted to the fixed bed adsorptive reactors, in which the active packing consists of a mixture of a catalyst and sorbent particles – e.g. see some of the above cited papers [11, 15, 29, 34, 37, 17, 20–25, 27].

Apart from fixed bed reactors, also bubbling fluidized bed reactors employed to carry out SESMR process were investigated – here a series of papers by Jacobsen *et al.* [39, 41, 43, 47, 50] should be mentioned. In those papers, it has been proved numerically that in the bubbling fluidized bed, due to intensive mixing, axial temperature and concentration profiles are very smooth.

In a case of FA application, particles of very small size are used, so only a fluidized bed reactor or a gas-solid-solid trickle flow reactor can be employed.

To model the reactor of any type, the appropriate set of mass, heat, momentum and continuity balance equations should be formulated. A general reactor model, which takes into account all complex phenomena present in the system, can be significantly simplified according to the system characterization and operating conditions.

To demonstrate the main properties of the SESMR process, a calculation example is presented. The modeling and simulation results shown below, are for the fluidized bed gradienless reactor (FBGLR). This type of reactor has been chosen to indicate an operating conditions window for SESMR process, to determine an influence of process variables on the reactor performance as well as to estimate the feasibility of the chosen reactor type (operating mode).

A configuration of the reactor (FBGLR) is shown schematically in Fig. 4. In this reactor type the catalyst grains are fixed formulating a bed of large external porosity. In another solution the active catalyst sides can be immobilized inside large pore structured ceramic or metallic foams. Fine grains of the sorbent (particles of fly ashes as small as 3–5 μm) are continuously added into the reactor, then fluidize inside the reactor and are removed after a fixed residence time. The flow rates of fly ashes at the reactor inlet and outlet are the same.

Due to intensive stirring of gaseous phase and FA particles, perfect mixing conditions can be assumed. Additionally, external and internal mass and heat transfer resistances are neglected, so as a consequence the same temperature of reactor content (i.e. gaseous species and solid particles) and no concentration

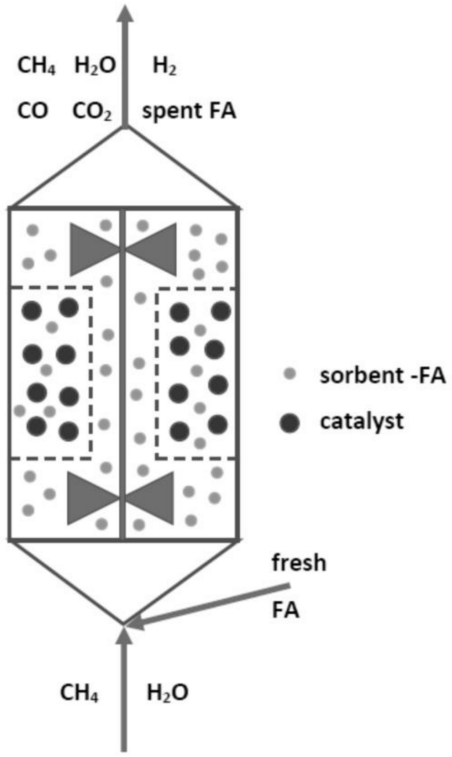

Fig. 4. Configuration of the fluidized bed gradientless reactor (FBGLR) employed to carry out the SESMR process with simultaneous sequestration of CO_2 on fly ashes

gradients of reactants in the gaseous phase considered. Also an applicability of the ideal gas law as well as a selectivity of the sorbent towards the CO_2 are assumed.

Then, for isothermal (T_R = const) and isobaric (P_R = const) reactor operating conditions, at the steady state the following model equations have been formulated:

- molar balance for the gaseous phase(general reactant mass balance)

$$\sum_{i=1}^{5} \Phi_0 \cdot y_{0,i} + \sum_{i=1}^{5} (r_{R,1} \cdot m_{\text{cat}}) - r_{S,4} \cdot m_S = \Phi \tag{26}$$

- molar balance for i-th reacting compound in the gas phase

$$\Phi_0 \cdot y_{0,i} + r_{R,i} \cdot m_{\text{cat}} - r_{S,i} \cdot m_{\text{FA}} = \Phi \cdot y_i \tag{27}$$

- molar balance of the CO_2 in the solid phase

$$\dot{m}_{\text{FA}} \cdot q_{0,4} + m_{\text{FA}} \cdot r_{S,4} = \dot{m}_{\text{FA}} \cdot q_4 \tag{28}$$

where each reacting species is denoted as: 1 – CH_4, 2 – H_2O, 3 – H_2, 4 – CO_2, 5 – CO, respectively. Because of selective sorption of CO_2, the sorption rates for other reacting species are always equal to zero – i.e. $r_{S,1} = r_{S,2} = r_{S,3} = r_{S,5} = 0$, while the CO_2 sorption rate – $r_{S,4}$ can be predicted from Eqs. (19) and (20), for CaO and FA, respectively.

Notice, that the sorbent loading (hold-up), $m_{\text{FA}} = m_S$ appearing above in balance equations, strongly depends on the operating conditions; mainly on the gas flow rate and stirrer speed. In contrast the catalyst loading – m_{cat} can be easily and independently changed from run to run, thus establishing the amount of the catalyst grains placed in the basket or changing the number of active sites immobilized on ceramic/metallic foam surface.

Due to assumed perfect mixing and isothermal operating conditions the heat balance is not taken into account in the presented reactor model.

Considering a stoichiometry of the reactions involved, conversion rates for each i-th reactant – $r_{R,i}$ (in Eqs. (26)–(28)), can be expressed in terms of reaction rates r_{I}, r_{II}, r_{III} (estimated by means of Eqs. (4)–(17)) giving:

$$r_{R,1} = -r_{\mathrm{I}} - r_{\mathrm{II}} \tag{29}$$

$$r_{R,2} = -r_{\mathrm{I}} - 2r_{\mathrm{II}} - r_{\mathrm{III}} \tag{30}$$

$$r_{R,3} = 3r_{\mathrm{I}} + 4r_{\mathrm{II}} + r_{\mathrm{III}} \tag{31}$$

$$r_{R,4} = r_{\mathrm{II}} + r_{\mathrm{III}} \tag{32}$$

$$r_{R,5} = r_{\mathrm{I}} - r_{\mathrm{III}} \tag{33}$$

The formulated model equations (Eqs. (26)–(33)) have been implemented within the MatLab software environment and solved for the following inlet conditions:

$$y_{0,i} = \frac{\Phi_{0,i}}{\sum_{i=1}^{5} \Phi_{0,i}} \tag{34}$$

with the chosen values of the inlet molar flow rates of methane and steam: $\Phi_{0,1}$, $\Phi_{0,2} = s\Phi_{0,1}$, respectively. For the rest of reacting compounds we have: $\Phi_{0,3} = \Phi_{0,4} = \Phi_{0,5} = 0$ and the inlet concentration of CO_2 adsorbed on FA is also equal to zero: $q_{0,4} = 0$.

During model calculations the value of the CO_2 uptake coefficient – γ should be observed, as the CO_2 sorption rate $r_{S,4}$ becomes equal to zero if fly ashes present in the reactor are saturated with CO_2. This determines the maximum average residence time for fly ashes particles inside the reactor (saturation time) – τ_{sat}, which can be estimated from the following relationship:

$$\gamma_{\mathrm{sat}} = M_{\mathrm{CO2}} \int_0^{\tau_{\mathrm{sat}}} r_{s,4} dt = 0.035 \tag{35}$$

Notice that the CO_2 uptake coefficient – γ can be directly related to the outlet concentration – q_4 determined with the model, as the following relationship always holds: $\gamma = q_4 M_{\mathrm{CO2}}$.

So, at a given loading of the reactor with fly ashes (sorbent hold-up) – $m_{\mathrm{FA}} = m_{\mathrm{S}}$, the minimum effective mass flow rate of fly ashes flowing through the reactor can be directly determined as:

$$\dot{m}_{\mathrm{FA,min}} = \frac{m_{\mathrm{FA}}}{\tau_{\mathrm{sat}}} \tag{36}$$

For any flow rate of FA smaller than $\dot{m}_{\mathrm{FA,min}}$ the average residence time of the sorbent inside the reactor is too long, so the saturated particles of fly ashes are not able to adsorb more CO_2 and hydrogen productivity deteriorates.

Some representative results of performed simulations are presented in Figs. 5–9, where values of the most important process variables (process efficiency measures) are displayed: – Y_3, Y_4, Y_5 ("dry-basis" molar fraction of H_2, CO_2 and CO, respectively in the outlet gas stream), – ζ_1 (conversion of CH_4), – $\Phi_3/\Phi_{\mathrm{o},1}$ (reactor productivity measured as the ratio of the output H_2 to the input CH_4 molar flow rates). To this end, the molar concentration of each reacting compound in the outlet gas stream – y_i has been recalculated into the so-called "dry basis" molar fraction – Y_i following the relationship: $Y_i = y_i/(1 - y_2)$, where y_2 is the molar fraction of unreacted steam present in the outlet gas stream. Thus, the values of Y_i describe the molar fraction of i-th compound in the outlet gas stream after condensation of the unreacted excess steam.

A comparison of the reactor performance depending on the sorbent type is given in Fig. 5, where results obtained for two runs carried out at the same operating conditions but for two different CO_2 sorbents: CaO and FA are given.

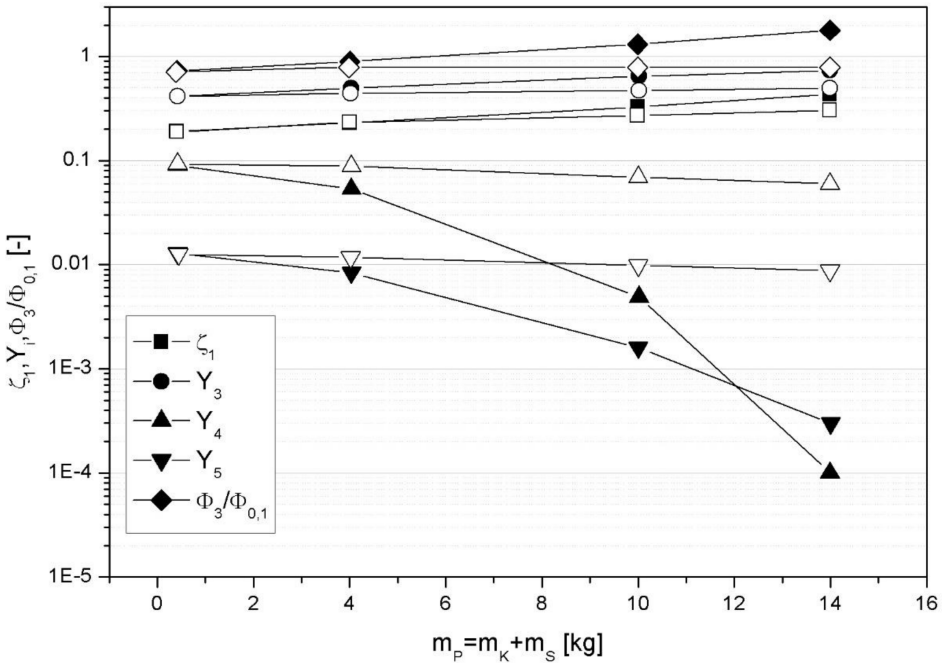

Fig. 5. Performance of the FBGLR for different CO_2 sorbents; CaO and FA, respectively CaO – full symbols, FA – open symbols. Reactor operating conditions: $V_R = 0.1$ m^3, $m_{cat}/m_S = 1$, $T = 773$ K, $P = 2$ bar, $s = 2$, $\Phi_{0,1} = 200$ mol/h

A set of process efficiency measures: Y_3, Y_4, Y_5, ζ_1, $\Phi_3/\Phi_{o,1}$ is displayed in Fig. 5 as a function of the total reactor loading $m_P = m_{cat} + m_S$, for CaO and for FA, respectively.

The obtained results indicate that for both, CaO and FA, sorbents the behavior of the reactor is similar. However, at higher total reactor loading m_P more distinctive differences are visible – i.e. smaller outlet concentrations of CO and CO_2 (Y_4 and Y_5) and higher outlet concentration of H_2 (Y_3), methane conversion (ζ_1) and ratio $\Phi_3/\Phi_{o,1}$. It is probably because of a higher CO_2 sorption rate for CaO than that for FA at a chosen temperature of process – see Eqs. (19) and (20), respectively.

Temperature influence on the reactor performance is shown in Fig. 6. An increase of the reactor temperature causes an increase of all used reactor efficiency measures. An increase of Y_3, ζ_1 and $\Phi_3/\Phi_{o,1}$ is profitable, while an increase of Y_4 and Y_5 is rather undesirable. However,these concentrations are still acceptable from the reactor performance point of view. The observed effect can be caused by the fact that temperature increase favors stronger the reaction kinetics than the sorption kinetics and that in this reactor type an increase of the temperature decreases the residence time of gaseous reactants.

An influence of the catalyst to sorbent mass ratio – m_{cat}/m_S on the reactor performance is shown in Fig. 7. It can be observed that for the chosen values of the ratio: $0.08 < m_{cat}/m_{FA} < 1$ no significant changes in the reactor performance are noticed.

An influence of the molar excess of water (steam) in the inlet gas stream – s and the reactor pressure – P is shown in Figs. 8 and 9, respectively. An increase of the water excess in the inlet stream – s improves the reactor performance – i.e. it causes an increase of the methane conversion – ζ_1 and the outlet hydrogen concentration – Y_3, while the concentrations of CO and CO_2 in the outlet gas stream only slightly increase.

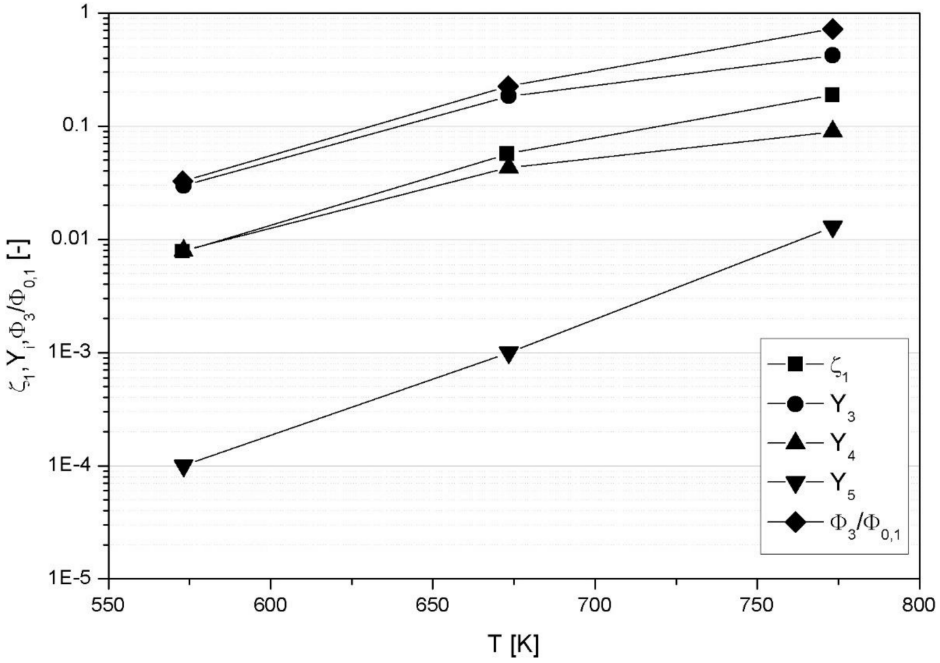

Fig. 6. Performance of the FBGLR with FA as the CO_2 sorbent – influence of the reactor temperature. Reactor operating conditions: $V_R = 0.1$ m^3, $m_{cat} = 7$ kg, $m_S = 7$ kg, $T = 773$ K, $P = 2$ bar, $s = 2$, $\Phi_{0,1} = 200$ mol/h

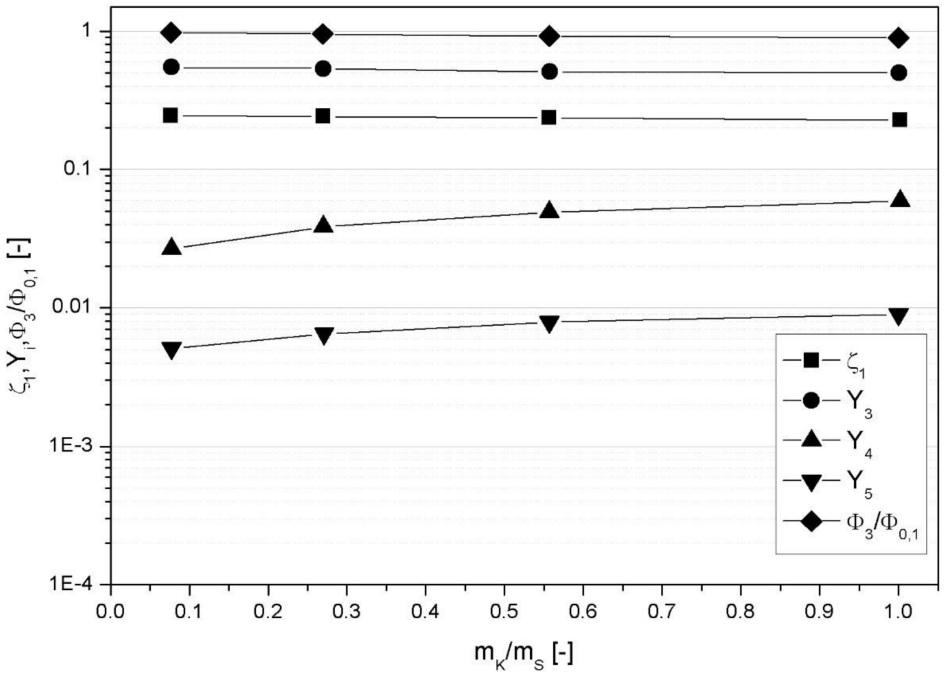

Fig. 7. Performance of the FBGLR with FA as the CO_2 sorbent – influence of the ratio $R = m_{cat}/m_{FA}$. Reactor operating conditions: $V_R = 0.1$ m^3, $m_P = m_{cat} + m_S = 14$ kg, $T = 773$ K, $P = 2$ bar, $s = 2$, $\Phi_{0,1} = 200$ mol/h

This can be caused by a combined effect of the parameter s, as its increase stimulates significantly the reaction rates, but in parallel the residence time of reactants in the reactor decreases.

An influence of the reactor pressure – P is shown in Fig. 9. An increase of P very slightly deteriorates the methane conversion – ζ_1, the hydrogen concentration – Y_3 and the hydrogen productivity – $\Phi_3/\Phi_{o,1}$, while CO and CO_2 concentrations – Y_4, Y_5 significantly decrease.

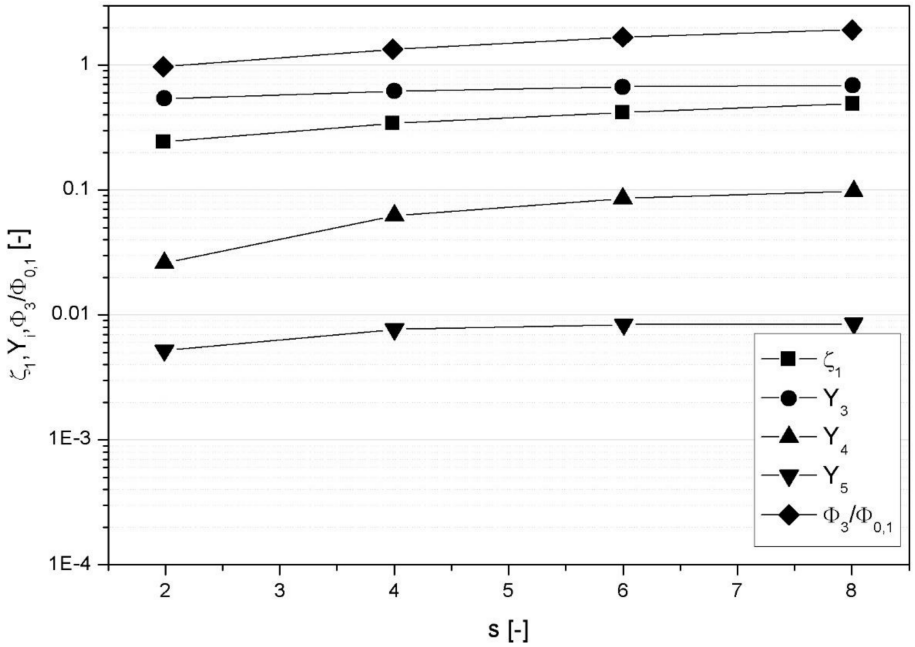

Fig. 8. Performance of the FBGLR with FA as the CO_2 sorbent – influence of the water excess – s. Reactor operating conditions: $V_R = 0.1$ m^3, $m_P = m_{cat} + m_S = 14$ kg, $R = m_{cat}/m_{FA} = 1/13$, $T = 773$ K, $P = 2$ bar, $\Phi_{0,1} = 200$ mol/h

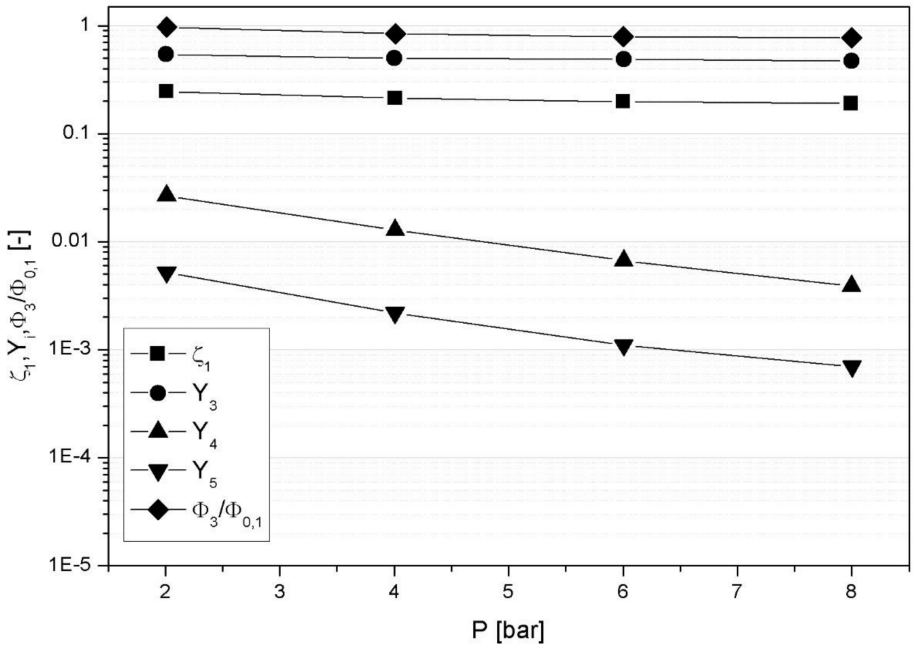

Fig. 9. Performance of the FBGLR with FA as the CO_2 sorbent – influence of the reactor pressure – P Reactor operating conditions: $V_R = 0.1$ m^3, $m_P = m_{cat} + m_S = 14$ kg, $R = m_{cat}/m_{FA} = 1/13$, $T = 773$ K, $s = 2$, $\Phi_{0,1} = 200$ mol/h

An influence of the residence time of gaseous reactants on the reactor performance has been also investigated (the results are not shown in diagrams). It has been found that a simple decrease of gas flow rates at the reactor inlet significantly improves both, the effectiveness as well as concentration measures, although the reactor productivity of course decreases.

Due to a specific operating mode the FBGLR is not dedicated to carry out effectively the SESMR process. However, all the results shown in Figs. 5-9 obtained for the sorption enhanced process have been compared

to the results obtained at the same operating conditions but without the presence of sorbent and always the efficiency for SESMR process was better than for a conventional SMR process.

The obtained results, despite the simplifications assumed – i.e. mainly isothermal operating conditions and no mass and heat transfer resistance - enable to understand the behavior of such a complex reacting-adsorption system and they supply indications for further experimental investigations in a larger scale.

As mentioned above, for FBGLR the very important process parameter is the hold-up of fly ash particles present in the reactor as well as its dependence on the operating conditions, particularly on gas flow rates. As far as we know, in the literature there is no data on this subject, especially for large scale systems working under elevated pressure and in the presence of steam.

4. SUMMARY AND CONCLUSIONS

In this review intensive studies on the sorption-enhanced steam methane reforming (SESMR) process dedicated to production of pure hydrogen have been presented and discussed. It should be pointed out that the catalysts to carry out this process are very well established and usually Ni-based catalysts applied for conventional SMR process are employed. However, also new active catalysts, e.g. Rh and Rh-Zr-based [34–36], are still being developed and tested.

The main problem for efficient execution of the SESMR process as well as its successful implementation in industrial practice are appropriate CO_2 sorbents. Sorbents used in the SESMR process for simultaneous CO_2 sorption have to meet several conditions – among others: – appropriate sorption rate compatible to the reaction rate (CO_2 production rate), – high sorption capacity, – mechanical, chemical and thermal durability. Numerous papers report results of sorbent investigations and the following sorbent groups can be distinguished: – CaO-based sorbents and alkali-modified hydrotalcities, – lithium oxides and lithium containing materials, – fly ashes from power plants. Recently, some investigations are also devoted to elaboration of hybrid catalyst-sorbent structured materials [78].

The application of fly ashes (FA) seems to be a very attractive alternative to other sorbents, as they do not require regeneration [60, 82]. Application of FA can significantly simplify the SESMR process and improve ecological factors of hydrogen production. This concept has been experimentally proved. However, many investigations in the pilot and industrial scales are needed for commercialization of this concept.

A brief survey of rector types employed to carry out SESMR is also given. It can be concluded that while fixed bed reactors are mostly used, fluidized bed reactors are quite widely employed as well. While the investigations carried out with fixed bed reactors are mostly both experimental and theoretical ones, those concerning fluidized bed reactors are almost all theoretical. Obtained results show the influence of main process variables (reactor temperature and pressure, molar excess of steam in the inlet gas stream and loading of the reactor with catalyst and sorbent) on the performance of considered reactors.

This work has been partially carried out within the frame of the project financially supported by the National Centre of Science, Poland.

SYMBOLS

b_{CO2}	constant (Eq. (24)), 1/bar
$k_{S,CO2}$	sorption rate constant, 1/s

k_{I}	reaction rate constant (Eqs. (4), (15)), mol bar$^{0.5}$/(kg$_{\mathrm{cat}}$ h)
k_{II}	reaction rate constant (Eqs. (5), (16)), mol bar $^{0.5}$/(kg$_{cat}$ h)
k_{III}	reaction rate constant (Eqs. (6), (17)), mol /(kg$_{cat}$ bar h)
K_1	constant (Eqs. (7), (8)), 1/bar
K_2	constant (Eqs. (7), (9)), –
K_3	constant (Eq. (7), (10)), 1/bar
K_5	constant (Eq. (7), (11)), 1/bar
K_{I}	chemical equilibrium constant (Eq. 4, 12), bar^2
K_{II}	chemical equilibrium constant (Eq. 5, 14), –
K_{III}	chemical equilibrium constant (Eq. 6, 13), bar^2
$K_{eq,1}$, $K_{eq,2}$	equilibrium constants (Eq. (25)), 1/bar
m_{CO2}	constant (Eq. (24)), mol/kg
m_{cat}	mass of the catalyst, kg
$m_{\mathrm{S}} = m_{\mathrm{FA}}$	mass of the sorbent, kg
$m_{\mathrm{P}} = m_{\mathrm{S}} + m_{\mathrm{cat}}$	mass of solid inserts, kg
$\dot{m}_{\mathrm{FA}}$	mass flow rate of the adsorbent (FA) through the reactor, kg/s
M_{CO2}	molar mass of CO_2, kg/mol
P	pressure, MPa
p_i	partial pressure of i-th compound (Eq. (4)–(6)), bar
q_4	molar concentration of adsorbed CO_2, mol$_{\mathrm{CO2}}$/kg$_{\mathrm{FA}}$
$q_{\mathrm{CO2},eq}$	equilibrium CO_2 concentration in the sorbent, mol/kg
$\overline{q}_{\mathrm{CO2}}$	average concentration of adsorbed CO_2, mol/kg
$q_{\mathrm{max},1}$, $q_{\mathrm{max},2}$	maximal sorption capacity (Eq. (25)), mol/kg
r_{I}, r_{II}, r_{III}	reaction rate (Eq. (4)–(6)), mol/(kg$_{\mathrm{cat}}$ h)
$r_{R,i}$	conversion rate for i-th reactant, mol/(kg$_{\mathrm{cat}}$ s)
$r_{S,4}$	CO_2 adsorption rate, mol$_{\mathrm{CO2}}$/(kg$_{\mathrm{FA}}$s)
s	molar excess of steam in the inlet stream, –
V_{R}	volume of the gaseous phase, m^3
T	temperature, K
y_i	molar fraction of i-th gaseous compound, –
Y_i	molar fraction of i-th gaseous compound (dry-basis), –

Greek symbols

γ	CO_2 uptake coefficient, kg$_{\mathrm{CO2}}$/kg$_{\mathrm{FA}}$
ΔH	reaction enthalpy, kJ/ mol
Φ	molar flow rate of gas, mol/s

Abbreviations and subscripts

Compounds:	1 – CH_4, 2 – H_2O, 3 – H_2, 4 – CO_2, 5 – CO
SESMR	sorption-enhanced steam-methane reforming
FBGLR	fluidized bed gradientless reactor
GSSTFR	gas-solid-solid trickle flow reactor
cat	catalyst
FA	fly ashes
S	sorbent
R	reactor
o	initial

REFERENCES

1. IEA, 2012. *Energy Technology Perspectives 2012: Pathways to a Clean Energy System.* OECD Publishing, Paris. DOI: 10.1787/energy_tech-2012-en.
2. Muradov N., Vezirolu T., 2005. From hydrocarbon to hydrogen-carbon to hydrogen economy. *Int. J. Hydrogen Energy*, 30, 225–237. DOI: 10.1016/j.ijhydene.2004.03.033.
3. Hufton J.R.R., Mayorga S., Sircar S., 1999. Sorption-enhanced reaction process for hydrogen production. *AIChE J.*, 45, 248–256. DOI: 10.1002/aic.690450205.
4. Agar D.W., 2005. The dos and don'ts of adsorptive reactors, In: Sundmacher K., Kienle A., Seidel-Morgenstern A., *Integrated Chemical Processes: Synthesis, Operation, Analysis, and Control*. Wiley-VCH Verlag GmbH & Co. KGaA, 203–232. DOI: 10.1002/3527605738.ch7.
5. Molga E., 2008. *Reactive adsorption processes – Adsorptive and chromatographic reactors*. WNT, Warszawa (in Polish).
6. Sircar S., Lee K.B. (Eds.), 2010. *Sorption enhanced reaction concepts for hydrogen production: Materials & processes*. Research Singpost.
7. Wu Y.-J., Li P., Yu J.-G., Cunha A.F., Rodrigues A.E., 2016. Progress on sorption-enhanced reaction process for hydrogen production. *Rev. Chem. Eng.*, 32, 271–303. DOI: 10.1515/revce-2015-0043.
8. Harrison D.P., 2008. Sorption-enhanced hydrogen production: A review. *Ind. Eng. Chem. Res.*, 47, 6486–6501. DOI: 10.1021/ie800298z.
9. Rodrigues A.E., Madeira L.M., Wu Y.-J., Faria R., 2017. *Sorption enhanced reaction processes*, Vol. 01. Portugal World Scientific (Europe). DOI: 10.1142/q0103.
10. Waldron W.E.E., Hufton J.R.R., Sircar S., 2001. Production of hydrogen by cyclic sorption enhanced reaction process. *AIChE J.*, 47, 1477–1479. DOI: 10.1002/aic.690470623.
11. Xiu G., Li P., Rodrigues A.E., 2003. Adsorption-enhanced steam-methane reforming with intraparticle-diffusion limitations. *Chem. Eng. J.*, 95, 83–93. DOI: 10.1016/S1385-8947(03)00116-5.
12. Carvill B.T.T., Hufton J.R.R., Anand M., Sircar S., 1996. Sorption-enhanced reaction process. *AIChE J.*, 42, 2765–2772. DOI: 10.1002/aic.690421008.
13. Balasubramanian B., Lopez Ortiz A., Kaytakoglu S., Harrison D.P., 1999. Hydrogen from methane in a single-step process. *Chem. Eng. Sci.*, 54, 3543–3552. DOI: 10.1016/S0009-2509(98)00425-4.
14. Ding Y., Alpay E., 2000. Equilibria and kinetics of CO_2 adsorption on hydrotalcite adsorbent. *Chem. Eng. Sci.*, 55, 3461–3474. DOI: 10.1016/S0009-2509(99)00596-5.
15. Ding Y., Alpay E., 2000. Adsorption-enhanced steam–methane reforming. *Chem. Eng. Sci.*, 55, 3929–3940. DOI: 10.1016/S0009-2509(99)00597-7.
16. Zou Y., Rodrigues A.E., 2001. The separation enhanced reaction process (SERP) in the production of hydrogen from methane steam reforming. *Adsorpt. Sci. Technol.*, 19, 655–671. DOI: 10.1260/0263617011494475.
17. Chanburanasiri N., Ribeiro A.M., Rodrigues A.E., Laosiripojana N., Assabumrungrat S., 2013. Simulation of methane steam reforming enhanced by in situ CO_2 sorption using K_2CO_3-promoted hydrotalcites for H_2 production. *Energy Fuels*, 27, 4457–4470. DOI: 10.1021/ef302043e.
18. Oliveira E.L.G., Grande C.A., Rodrigues A.E., 2008. CO_2 sorption on hydrotalcite and alkali-modified (K and Cs) hydrotalcites at high temperatures. *Sep. Purif. Technol.*, 62, 137–147. DOI: 10.1016/j.seppur.2008.01.011.
19. Wang Y.-N., Rodrigues A.E., 2005. Hydrogen production from steam methane reforming coupled with in situ CO_2 capture: Conceptual parametric study. *Fuel*, 84, 1778–1789. DOI: 10.1016/j.fuel.2005.04.005.
20. Xiu G.H., Li P., Rodrigues A.E., 2004. Subsection-controlling strategy for improving sorption-enhanced reaction process. *Chem. Eng. Res. Des.*, 82, 192–202. DOI: 10.1205/026387604772992765.
21. Xiu G., Li P., Rodrigues A.E., 2003. New generalized strategy for improving sorption-enhanced reaction process. *Chem. Eng. Sci.*, 58, 3425–3437. DOI: 10.1016/S0009-2509(03)00200-8.

22. Xiu G., Soares J.L., Li P., Rodrigues A.E., 2002. Simulation of five-step one-bed sorption-enhanced reaction process. *AIChE J.*, 48, 2817–2832. DOI: 10.1002/aic.690481210.

23. Xiu G., Li P., E. Rodrigues A., 2002. Sorption-enhanced reaction process with reactive regeneration. *Chem. Eng. Sci.*, 57, 3893–3908. DOI: 10.1016/S0009-2509(02)00245-2.

24. Rusten H.K., Ochoa-Fernández E., Lindborg H., Chen D., Jakobsen H.A., 2007. Hydrogen production by sorption-enhanced steam methane reforming using lithium oxides as CO_2-acceptor. *Ind. Eng. Chem. Res.*, 46, 8729–8737. DOI: 10.1021/ie070770k.

25. Rusten H.K., Ochoa-Fernández E., Chen D., Jakobsen H.A., 2007. Numerical investigation of sorption enhanced steam methane reforming using Li_2ZrO_3 as CO_2-acceptor. *Ind. Eng. Chem. Res.*, 46, 4435–4443. DOI: 10.1021/ ie061525o.

26. Ochoa-Fernández E., Haugen G., Zhao T., Rřnning M., Aartun I., Břrresen B., Rytter E., Rřnnekleiv M., Chen D., 2007. Process design simulation of H_2 production by sorption enhanced steam methane reforming: evaluation of potential CO_2 acceptors. *Green Chem.*, 9, 654–662. DOI: 10.1039/B614270B.

27. Ochoa-Fernández E., Rusten H.K., Jakobsen H.A., Rřnning M., Holmen A., Chen D., 2005. Sorption enhanced hydrogen production by steam methane reforming using Li2ZrO3 as sorbent: Sorption kinetics and reactor simulation. *Catal. Today*, 106, 41–46. DOI: 10.1016/j.cattod.2005.07.146.

28. Reijers H.T.J., Elzinga G.D., Cobden P.D., Haije W.G., van den Brink R.W., 2011. Tandem bed configuration for sorption-enhanced steam reforming of methane. *Int. J. Greenh. Gas Control*, 5, 531–537. DOI: 10.1016/j.ijggc. 2010.04.007.

29. Reijers H.T.J., Boon J., Elzinga G.D., Cobden P.D., Haije W.G., van den Brink R.W., 2009. Modeling study of the sorption-enhanced reaction process for CO_2 capture. I. Model development and validation. *Ind. Eng. Chem. Res.*, 48, 6966–6974. DOI: 10.1021/ie801319q.

30. Reijers H.T.J., Boon J., Elzinga G.D., Cobden P.D., Haije W.G., van den Brink R.W., 2009. Modeling study of the sorption-enhanced reaction process for CO_2 Capture. II. Application to steam-methane reforming. *Ind. Eng. Chem. Res.*, 48, 6975–6982. DOI: 10.1021/ie8013204.

31. Solieman A.A.A., Dijkstra J.W., Haije W.G., Cobden P.D., van den Brink R.W., 2009. Calcium oxide for CO_2 capture: Operational window and efficiency penalty in sorption-enhanced steam methane reforming. *Int. J. Greenh. Gas Control*, 3, 393–400. DOI: 10.1016/j.ijggc.2009.02.002.

32. Cobden P.D., van Beurden P., Reijers H.T.J., Elzinga G.D., Kluiters S.C.A., Dijkstra J.W., Jansen D., van den Brink R.W., 2007. Sorption-enhanced hydrogen production for pre-combustion CO_2 capture: Thermodynamic analysis and experimental results. *Int. J. Greenh. Gas Control*, 1, 170–179. DOI: 10.1016/S1750-5836(07) 00021-7.

33. Reijers H.T.J., Valster-Schiermeier S.E.A.A., Cobden P.D., van den Brink R.W., 2006. Hydrotalcite as CO_2 sorbent for sorption-enhanced steam reforming of methane. *Ind. Eng. Chem. Res.*, 45, 2522–2530. DOI: 10.1021/ ie050563p.

34. Halabi M.H., de Croon M.H.J.M., van der Schaaf J., Cobden P.D., Schouten J.C., 2012. Kinetic and structural requirements for a CO_2 adsorbent in sorption enhanced catalytic reforming of methane – Part I: Reaction kinetics and sorbent capacity. *Fuel*, 99, 154–164. DOI: 10.1016/j.fuel.2012.04.016.

35. Halabi M.H., de Croon M.H.J.M., van der Schaaf J., Cobden P.D., Schouten J.C., 2012. A novel catalyst–sorbent system for an efficient H_2 production with in-situ CO_2 capture. *Int. J. Hydrogen Energy*, 37, 4987–4996. DOI: 10.1016/j.ijhydene.2011.12.025.

36. Halabi M.H., de Croon M.H.J.M., van der Schaaf J., Cobden P.D., Schouten J.C., 2012. High capacity potassium-promoted hydrotalcite for CO_2 capture in H_2 production. *Int. J. Hydrogen Energy*, 37, 4516–4525. DOI: 10.1016/ j.ijhydene.2011.12.003.

37. Halabi M.H., de Croon M.H.J.M., van der Schaaf J., Cobden P.D., Schouten J.C., 2011. Reactor modeling of sorption-enhanced autothermal reforming of methane. Part I: Performance study of hydrotalcite and lithium zirconate-based processes. *Chem. Eng. J.*, 168, 872–882. DOI: 10.1016/j.cej.2011.02.015.

38. Halabi M.H., de Croon M.H.J.M., van der Schaaf J., Cobden P.D., Schouten J.C., 2011. Reactor modeling of sorption-enhanced autothermal reforming of methane. Part II: Effect of operational parameters. *Chem. Eng. J.*, 168, 883–888. DOI: 10.1016/j.cej.2011.02.016.

39. Chao Z., Zhang Y., Wang Y., Jakobsen J.P., Jakobsen H.A., 2017. Modelling of binary fluidized bed reactors for the sorption-enhanced steam methane reforming process. *Can. J. Chem. Eng.*, 95, 157–169. DOI: 10.1002/cjce.22602.

40. Solsvik J., Chao Z., Jakobsen H.A., 2015. Modeling and simulation of bubbling fluidized bed reactors using a dynamic one-dimensional two-fluid model: The sorption-enhanced steam–methane reforming process. *Adv. Eng. Softw.*, 80, 156–173. DOI: 10.1016/j.advengsoft.2014.09.011.

41. Solsvik J., Chao Z., Sánchez R.A., Jakobsen H.A., 2014. Numerical investigation of steam methane reforming with CO_2-capture in bubbling fluidized bed reactors. *Fuel Process. Technol.*, 125, 290–300. DOI: 10.1016/j.fuproc.2014.03.039.

42. Wang J., Wang Y., Jakobsen H.A., 2014. The modeling of circulating fluidized bed reactors for SE-SMR process and sorbent regeneration. *Chem. Eng. Sci.*, 108, 57–65. DOI: 10.1016/j.ces.2013.12.012.

43. Solsvik J., Sánchez R.A., Chao Z., Jakobsen H.A., 2013. Simulations of steam methane reforming/sorption-enhanced steam methane reforming bubbling fluidized bed reactors by a dynamic one-dimensional two-fluid model: Implementation issues and model validation. *Ind. Eng. Chem. Res.*, 52, 4202–4220. DOI: 10.1021/ie303348r.

44. Rout K.R., Jakobsen H.A., 2013. A numerical study of pellets having both catalytic- and capture properties for SE-SMR process: Kinetic- and product layer diffusion controlled regimes. *Fuel Process. Technol.*, 106, 231–246. DOI: 10.1016/j.fuproc.2012.07.029.

45. Rout K.R., Jakobsen H.A., 2012. Reactor performance optimization by the use of a novel combined pellet reflecting both catalyst and adsorbent properties. *Fuel Process. Technol.*, 99, 13–34. DOI: 10.1016/j.fuproc.2012.01.035.

46. Solsvik J., Jakobsen H.A., 2011. A numerical study of a two property catalyst/sorbent pellet design for the sorption-enhanced steam–methane reforming process: Modeling complexity and parameter sensitivity study. *Chem. Eng. J.*, 178, 407–422. DOI: 10.1016/j.cej.2011.10.045.

47. Rout K.R., Solsvik J., Nayak A.K., Jakobsen H.A., 2011. A numerical study of multicomponent mass diffusion and convection in porous pellets for the sorption-enhanced steam methane reforming and desorption processes. *Chem. Eng. Sci.*, 66, 4111–4126. DOI: 10.1016/j.ces.2011.05.040.

48. Wang Y., Chao Z., Jakobsen H.A., 2011. Numerical study of hydrogen production by the sorption-enhanced steam methane reforming process with online CO_2 capture as operated in fluidized bed reactors. *Clean Technol. Environ. Policy*, 13, 559–565. DOI: 10.1007/s10098-011-0368-y.

49. Wang Y., Chao Z., Jakobsen H.A., 2011. Effects of gas–solid hydrodynamic behavior on the reactions of the sorption enhanced steam methane reforming process in bubbling fluidized bed reactors. *Ind. Eng. Chem. Res.*, 50, 8430–8437. DOI: 10.1021/ie102330d.

50. Wang Y., Chao Z., Chen D., Jakobsen H.A., 2011. SE-SMR process performance in CFB reactors: Simulation of the CO_2 adsorption/desorption processes with CaO based sorbents. *Int. J. Greenh. Gas Control*, 5, 489–497. DOI: 10.1016/j.ijggc.2010.09.001.

51. Wang Y., Chao Z., Jakobsen H.A., 2010. 3D simulation of bubbling fluidized bed reactors for sorption enhanced steam methane reforming processes. *J. Nat. Gas Sci. Eng.*, 2, 105–113. DOI: 10.1016/j.jngse.2010.04.004.

52. Lindborg H., Jakobsen H.A., 2009. Sorption enhanced steam methane reforming process performance and bubbling fluidized bed reactor design analysis by use of a two-fluid model. *Ind. Eng. Chem. Res.*, 48, 1332–1342. DOI: 10.1021/ie800522p.

53. Chanburanasiri N., Ribeiro A.M., Rodrigues A.E., Arpornwichanop A., Laosiripojana N., Praserthdam P., Assabumrungrat S., 2011. Hydrogen production via sorption enhanced steam methane reforming process using Ni/CaO multifunctional catalyst. *Ind. Eng. Chem. Res.*, 50, 13662–13671. DOI: 10.1021/ie201226j.

54. Lugo E.L., Wilhite B.A., 2016. A theoretical comparison of multifunctional catalyst for sorption-enhanced reforming process. *Chem. Eng. Sci.*, 150, 1–15. DOI: 10.1016/j.ces.2016.04.011.

55. Aloisi I., Jand N., Stendardo S., Foscolo P.U., 2016. Hydrogen by sorption enhanced methane reforming: A grain model to study the behavior of bi-functional sorbent-catalyst particles. *Chem. Eng. Sci.*, 149, 22–34. DOI: 10.1016/ j.ces.2016.03.042.

56. Voldsund M., Jordal K., Anantharaman R., 2016. Hydrogen production with CO_2 capture. *Int. J. Hydrogen Energy*, 41, 4969–4992. DOI: 10.1016/j.ijhydene.2016.01.009.

57. Oliveira E.L.G., Grande C.A., Rodrigues A.E., 2011. Effect of catalyst activity in SMR-SERP for hydrogen production: Commercial vs. large-pore catalyst. *Chem. Eng. Sci.*, 66, 342–354. DOI: 10.1016/j.ces.2010.10.030.

58. Lee D.K., Baek I.H., Yoon W.L., 2004. Modeling and simulation for the methane steam reforming enhanced by in situ CO_2 removal utilizing the CaO carbonation for H_2 production. *Chem. Eng. Sci.*, 59, 931–942. DOI: 10.1016/j.ces.2003.12.011.

59. Zhang Q., Shen C., Zhang S., Wu Y., 2016. Steam methane reforming reaction enhanced by a novel K_2CO_3-Doped Li_4SiO_4 sorbent: Investigations on the sorbent and catalyst coupling behaviors and sorbent regeneration strategy. *Int. J. Hydrogen Energy*, 41, 4831–4842. DOI: 10.1016/j.ijhydene.2015.12.116.

60. Cherbański R., Molga E., 2018. Sorption-enhanced steam-methane reforming with simultaneous sequestration of CO_2 on fly ashes – Proof of concept and simulations for gas-solid-solid trickle flow reactor. *Chem. Eng. Process. – Process Intensif.*, 124, 37–49. DOI: 10.1016/j.cep.2017.11.010.

61. Westerterp K.R., Kuczynski M., 1987. A model for a countercurrent gas–solid–solid trickle flow reactor for equilibrium reactions. The methanol synthesis. *Chem. Eng. Sci.*, 42, 1871–1885. DOI: 10.1016/0009-2509(87) 80134-3.

62. Kuczynski M., Oyevaar M.H., Pieters R.T., Westerterp K.R., 1987. Methanol synthesis in a countercurrent gas–solid–solid trickle flow reactor. An experimental study. *Chem. Eng. Sci.*, 42, 1887–1898. DOI: 10.1016/0009-2509(87)80135-5.

63. Dallos C.G., Kafarov V., Filho R.M., 2007. A two dimensional steady-state model of the gas–solid–solid reactor. *Chem. Eng. J.*, 134, 209–217. DOI: 10.1016/j.cej.2007.03.044.

64. Dehghani Z., Bayat M., Rahimpour M.R., 2014. Sorption-enhanced methanol synthesis: Dynamic modeling and optimization. *J. Taiwan Inst. Chem. Eng.*, 45, 1490–1500. DOI: 10.1016/j.jtice.2013.12.001.

65. Hamidi M., Samimi F., Rahimpour M.R., 2015. Dimethyl ether synthesis in a gas–solid–solid trickle flow reactor with continuous adsorbent regeneration. *J. Taiwan Inst. Chem. Eng.*, 47, 105–112. DOI: 10.1016/j.jtice. 2014.10.013.

66. Bayat M., Hamidi M., Dehghani Z., Rahimpour M.R., 2014. Sorption-enhanced Fischer–Tropsch synthesis with continuous adsorbent regeneration in GTL technology: Modeling and optimization. *J. Ind. Eng. Chem.*, 20, 858–869. DOI: 10.1016/j.jiec.2013.06.016.

67. Bianchi E., Heidig T., Visconti C.G., Groppi G., Freund H., Tronconi E., 2012. An appraisal of the heat transfer properties of metallic open-cell foams for strongly exo-/endo-thermic catalytic processes in tubular reactors. *Chem. Eng. J.*, 198–199, 512–528. DOI: 10.1016/j.cej.2012.05.045.

68. Della Torre A., Lucci F., Montenegro G., Onorati A., Dimopoulos Eggenschwiler P., Tronconi E., Groppi G., 2016. CFD modeling of catalytic reactions in open-cell foam substrates. *Comput. Chem. Eng.*, 92, 55–63. DOI: 10.1016/j.compchemeng.2016.04.031.

69. Oliveira E.L.G.G., Grande C.A., Rodrigues A.E., 2009. Steam methane reforming in a Ni/Al_2O_3 catalyst: Kinetics and diffusional limitations in extrudates. *Can. J. Chem. Eng.*, 87, 945–956. DOI: 10.1002/cjce.20223.

70. Halabi M.H., de Croon M.H.J.M., van der Schaaf J., Cobden P.D., Schouten J.C., 2010. Low temperature catalytic methane steam reforming over ceria–zirconia supported rhodium. *Appl. Catal. A Gen.*, 389, 68–79. DOI: 10.1016/j.apcata.2010.09.004.

71. Dong W., 2002. Methane reforming over Ni/Ce-ZrO2 catalysts: effect of nickel content. *Appl. Catal. A Gen.*, 226, 63–72. DOI: 10.1016/S0926-860X(01)00883-3.

72. Roh H., 2002. Highly active and stable Ni/Ce–ZrO2 catalyst for H2 production from methane. *J. Mol. Catal. A Chem.*, 181, 137–142. DOI: 10.1016/S1381-1169(01)00358-2.

73. Takahashi R., Sato S., Sodesawa T., Yoshida M., Tomiyama S., 2004. Addition of zirconia in Ni/SiO_2 catalyst for improvement of steam resistance. *Appl. Catal. A Gen.*, 273, 211–215. DOI: 10.1016/j.apcata.2004.06.033.

74. Ochoa-Fernández E., Lacalle-Vilí C., Christensen K.O., Walmsley J.C., Rřnning M., Holmen A., Chen D., 2007. Ni catalysts for sorption enhanced steam methane reforming. *Top. Catal.*, 45, 3–8. DOI: 10.1007/s11244-007-0231-x.

75. Xu J., Froment G.F., 1989. Methane steam reforming, methanation and water-gas shift: I. Intrinsic kinetics. *AIChE J.*, 35, 88–96. DOI: 10.1002/aic.690350109.

76. Yong Z., Mata V., Rodrigues A., 2002. Adsorption of carbon dioxide at high temperature – A review. *Sep. Purif. Technol.*, 26, 195–205. DOI: 10.1016/S1383-5866(01)00165-4.

77. Yong Z., Rodrigues A.E., 2002. Hydrotalcite-like compounds as adsorbents for carbon dioxide. *Energy Convers. Manag.*, 43, 1865–1876. DOI: 10.1016/S0196-8904(01)00125-X.

78. Shokrollahi Yancheshmeh M., Radfarnia H.R., Iliuta M.C., 2016. High temperature CO_2 sorbents and their application for hydrogen production by sorption enhanced steam reforming process. *Chem. Eng. J.*, 283, 420–444. DOI: 10.1016/j.cej.2015.06.060.

79. Dou B., Wang C., Song Y., Chen H., Jiang B., Yang M., Xu Y., 2016. Solid sorbents for in-situ CO_2 removal during sorption-enhanced steam reforming process: A review. *Renew. Sustain. Energy Rev.*, 53, 536–546. DOI: 10.1016/j.rser.2015.08.068.

80. Lopes F.V.S., Grande C.A., Ribeiro A.M., Oliveira E.L.G., Loureiro J.M., Rodrigues A.E., 2009. Enhancing capacity of activated carbons for hydrogen purification. *Ind. Eng. Chem. Res.*, 48, 3978–3990. DOI: 10.1021/ie801132t.

81. Uliasz-Bochenczyk A., Mokrzycki E., 2006. Fly ashes from polish power plants and combined heat and power plants and conditions of their application for carbon dioxide utilization. *Chem. Eng. Res. Des.*, 84, 837–842. DOI: 10.1205/cherd.05145.

82. Molga E., Cherbanski R., 2012. Hydrogen production integrated with simultaneous CO_2 sequestration on fly ashes from power plants. *Chem. Eng. Technol.*, 35, 539–546. DOI: 10.1002/ceat.201100207.

83. Olivares-Marín M., Drage T.C., Maroto-Valer M.M., 2010. Novel lithium-based sorbents from fly ashes for CO_2 capture at high temperatures. *Int. J. Greenh. Gas Control*, 4, 623–629. DOI: 10.1016/j.ijggc.2009.12.015.

84. Wee J.-H., 2013. A review on carbon dioxide capture and storage technology using coal fly ash. *Appl. Energy*, 106, 143–151. DOI: 10.1016/j.apenergy.2013.01.062.

85. Yan F., Jiang J., Zhao M., Tian S., Li K., Li T., 2015. A green and scalable synthesis of highly stable Ca-based sorbents for CO_2 capture. *J. Mater. Chem. A*, 3, 7966–7973. DOI: 10.1039/C4TA06639A.

86. Sanna A., Ramli I., Mercedes Maroto-Valer M., 2015. Development of sodium/lithium/fly ash sorbents for high temperature post-combustion CO_2 capture. *Appl. Energy*, 156, 197–206. DOI: 10.1016/j.apenergy.2015.07.008.

87. Sanna A., Maroto-Valer M.M., 2016. CO_2 capture at high temperature using fly ash-derived sodium silicates. *Ind. Eng. Chem. Res.*, 55, 4080–4088. DOI: 10.1021/acs.iecr.5b04780.

88. Sanna A., Maroto-Valer M.M., 2016. Potassium-based sorbents from fly ash for high-temperature CO_2 capture. *Environ. Sci. Pollut. Res.*, 23, 22242–22252. DOI: 10.1007/s11356-016-6378-x.

89. Sreenivasulu B., Sreedhar I., Reddy B.M., Raghavan K.V., 2017. Stability and carbon capture enhancement by coal-fly-ash-doped sorbents at a high temperature. *Energy Fuels*, 31, 785–794. DOI: 10.1021/acs.energyfuels.6b02721.

Received 21 August 2018
Received in revised form 12 October 2018
Accepted 15 October 2018